LONDON2007

P097

Tube-Wave Reflections in Cased Boreholes

D. Alexandrov (St.-Petersburg State University), B.M. Kashtan (St.-Petersburg State University), A.V. Bakulin (Shell International Exploration and Production Inc) & S.R. Ziatdinov* (St.-Petersburg State University)

SUMMARY

At low frequencies tube or Stoneley waves represent a dominant arrival propagating along boreholes. They can be excited by the source in a well or by external source due to conversion from other wave types. Tube wave experiences reflection at the bed boundaries, borehole diameter changes and fractures or permeable zones. It was proven in previous studies that 1D effective wavenumber approach provides simple and accurate low-frequency description tube-wave propagation in open boreholes surrounded by radially homogeneous formation. Tube waves become even more dominant in cased boreholes, but casing further modifies wave propagation and reflection/transmission phenomena. In this study we apply 1D effective wavenumber approach to radially inhomogeneous media and demonstrate that it still provides excellent description of low-frequency tube-wave propagation. In particular, we focus on three models representative of cased boreholes: reflection from geological interfaces behind casing, reflection from corroded casing section and reflection from idealized disk-shaped perforation in cased hole. In all three cases frequency-dependent reflection coefficient obtained by 1D effective method and by finite-difference computations show excellent agreement.

Introduction

Tube (Stoneley) waves are useful for characterizing near-wellbore space since they are sensitive to borehole diameter changes, variations in elastic properties and permeability of the surrounding formations. In open-hole acoustic logging higher-frequency tube waves are used to detect and characterize fractures as well as to obtain a permeability profile (Winkler et al., 1989; Krauklis, 2005). In cased boreholes low-frequency tube-wave reflections can be used for estimation of quality and parameters of hydraulic fractures (Medlin and Schmitt, 1994; Paige et el., 1995) as well as other purposes. We are interested in the latter applications for cased boreholes where surrounding media is radially inhomogeneous (casing, cement, formation). Currently only numerical finite-difference methods can handle the reflection/transmission problem for such systems. Finite-difference method provides little physical insight into the problem. Approximate methods are useful for gaining better understanding of the problem of tube-wave reflections in cased boreholes. In this study we utilize 1D effective wavenumber approach suggested by White (1983) and extended by Tang and Cheng (1993). This approach was originally developed for low-frequency tube waves in radially homogeneous formations and was verified numerically for an open hole surrounded by elastic (Tezuka et al, 1997) and poroelastic formations (Bakulin et al., 2005). Here we extend this approach to radially imhomogeneous media with particular focus to cased boreholes.

1D effective wavenumber approach

Original formulation of 1D approach by White (1983) and later generalization by Tang and Cheng (1993) assumed radial homogeneity of the media surrounding the fluid column. This was appropriate to describe open-hole acoustic logging. While change in diameter (washout) could be treated, no radial layering was assumed beyond the fluid-formation interface. Our interest lies in analyzing interaction of tube waves with borehole structures in cased wells. Casing (and cement) represents another radial layer with very distinct parameters that substantially alters the properties of the tube wave (velocity, dispersion, attenuation) and ultimately modifies the reflection and transmission phenomena in an unknown manner. It seems that only numerical methods, like finite-difference, can correctly handle these interactions. Nevertheless, presence of elastic or poroelastic radial layering without additional fluid layers still supports only one propagating tube wave albeit with modified properties. Thus, it appears reasonable to assume that at least at low frequencies extension of 1D approach should still be applicable. Let us verify this hypothesis by means of a series of numerical tests.

First, let us remind the basics of 1D effective wavenumber approach (Tang and Cheng, 1993; Bakulin et al, 2005). In each homogeneous zone tube-wave propagation is described by a 1D wave equation with constant effective wavenumber that depends on the properties of the surrounding formation as well as geometrical borehole parameters and frequency. To obtain the amplitudes of upgoing and downgoing waves, mass-balance boundary conditions are set at each interface, in particular, continuity of the fluid pressure and of the fluid flow. Reflection and transmission coefficients from a single layer of any type are given by:

$$R = \frac{2i\left(k_2^2 - k_1^2\right)\sin(k_2 L)}{\left(k_1 + k_2\right)^2 e^{-ik_2 L} - \left(k_1 - k_2\right)^2 e^{ik_2 L}}, \quad T = \frac{4k_2 k_1 e^{-ik_1 L}}{\left(k_1 + k_2\right)^2 e^{-ik_2 L} - \left(k_1 - k_2\right)^2 e^{ik_2 L}}, \qquad (1)$$

where L is the layer thickness, k_1 *is* the axial Stoneley wavenumber in the two half-spaces and k_2 *is* the axial Stoneley wavenumber in the layer. These expressions are valid for a layer of any type as the rheology of the medium is absorbed by the effective wavenumber (Tang and Cheng, 1993). That is why we call this approach "effective wavenumber approach". Although equations (1) are obtained for homogeneous formation, we may apply them without modification for radially inhomogeneous formation, provided that Stoneley wavenumber is now computed for multi-layered model at hand. For simplicity in this study we assume radially layered model with three layers: fluid, casing and formation. In this case effective wavenumber k as a function of frequency is calculated numerically from set of equations

representing boundary conditions and assuming full bond between casing and formation. Once effective wavenumbers are established for each vertically homogeneous zone, equations (1) are used to compute the reflection coefficient as a function of frequency and compare them with the corresponding quantities found from finite difference modeling. Small tube-wave dispersion in cased boreholes allowed us to use frequency-independent velocities in all numerical examples below since computations with and without frequency dependence of the wavenumber are almost identical Material parameters for all models are summarized in Table 1.

Model 1: Reflection from geological interfaces behind casing

Figure 1 depicts first model when cased borehole penetrates two thin horizontal layers. At low frequencies these two layers generate a composite tube-wave reflection that can be computed using equations similar to (1) but generalized to a four-layered 1D model. Figure 2 shows a comparison of reflection coefficients obtained with 1D approach and a finite-difference code jointly developed by Keldysh Institute of Applied Mathematics and Shell. In the latter case reflection coefficients are estimated by taking spectral ratios of reflected and incident tube waveforms. Good agreement between the two sets of curves proves that the effective wavenumber approach does capture the most important features of tube-wave interactions with formations in cased boreholes. When softer (plastic) casing is used the tube-wave reflections are larger indicating increased sensitivity to variations of elastic parameters behind the casing as it is intuitively expected, while in case of steel casing this sensitivity is muted due to stronger containment of the tube wave.

Model 2: Reflection from corroded section of the casing

This section tests the 1D effective wavenumber approach for the case when variation in elastic parameters occurs in the properties of the first elastic layer - casing. The system under consideration is cased borehole surrounded by homogeneous formation (Figure 3). Casing has a corroded section with 0.8 m height. Density, longitudinal and shear velocities of corroded section are all reduced by the same multiplier Q (0.2, 0.5 and 0.7) compared to the properties of uncorroded section. Material parameters are given in the table below. Figure 4 confirms excellent agreement between approximate reflection coefficients obtained with 1D approach and ground truth response computed with finite-difference modeling. Notice that for reflection coefficient to become larger than 1%, elastic parameters of corroded region need to be reduced by at least factor of two.

Model 3: Idealized perforation in cased borehole

Given success in describing tube-wave interaction for cased borehole with constant radius, we decided to explore more complicated models with varying borehole diameter. In particular, we focus on "idealized perforation model" (Bakulin et al., 2005) depicted on Figure 5. While the material parameters in this model are identical to those for the corroded casing model of Figure 3 (except for corroded section), the key distinction is that instead of corroded region there is now disk-shaped perforation. Since formation is modeled as impermeable elastic space then effects related to fluid mobility between borehole and formation are neglected and only reflection due to geometric (diameter) changes are considered. Real perforation represents a small cylinder placed perpendicular to the main borehole in a particular azimuth and thus it will have much more limited area of fluid-formation interface. For this reason we call our model "idealized (disk-shaped) perforation". With all these limitations "idealized perforation model" is a useful first step since it can be easily treated by cylindrically symmetric approaches at hand: effective wavenumber scheme and radially symmetric elastic finite-difference code. Material parameters are given in the table below. Obtained reflection coefficients are given on Figure 6 and Figure 7 for the case of finite-length (0.1 m) and zero-length perforations respectively. The latter one represents case when there is only break in the casing but radius of formation interface remains constant. In both cases the height of the perforation was 0.8 m. Again agreement is excellent between 1D approach and finite-

difference numerical simulation. In case of a finite-length perforation (Figure 6) reflection is completely dominated by diameter change and is not dependent on casing parameters, whereas for zero-length perforation (Figure 7) steel casing leads to slightly higher reflection.

Conclusions

We extended 1D effective wavenumber approach to treat the interactions of low-frequency tube waves with various borehole structures in a radially inhomogeneous media that supports single tube-wave mode. In particular, we have shown good agreement between responses obtained with 1D approach and finite-difference computations in cased boreholes with vertical variation in properties of casing or formation layers. We further tested this method for simplest model of idealized (disk-shaped) perforation with no-flow boundary at the sand face. In this case change in diameter is additionally introduced. We predict that in case of poroelastic structures 1D effective wavenumber approach would also account for fluid flow effects and correctly describe tube-wave interaction with radially inhomogeneous permeable formations. Verification of this statement will be reported in future publications.

Table 1: Model parameters

Formation, casing and fluid properties	Elastic half-spaces	Casing 1 (steel)	Casing 2 (plastic)	Fluid
Longitudinal velocity v_p (m/s)	3500	6000	2840	1500
Shear velocity v_s (m/s)	2500	3000	1480	-
Density (kg/m^3)	3400	7000	1200	1000

Material properties of other layers	Layer 1	Layer 2	Corroded region 1	Corroded region 2	Corroded region 3
Longitudinal velocity v_p (m/s)	3100	3700	1200	3000	4200
Shear velocity v_s (m/s)	1800	2400	600	1500	2100
Density (kg/m^3)	2600	3000	1400	3500	4900

References

Bakulin, A., Gurevich, B., Ciz, R., and Ziatdinov S., [2005] Tube-wave reflection from a porous permeable layer with an idealized perforation. 75th Meeting, Society of Exploration Geophysicists, Expanded Abstract, 332-335.

Krauklis P.V., Krauklis A.P., [2005] Tube wave reflection and transmission on the fracture. 67th Conference & Exhibition. EAGE, Expanded abstracts. P217.

Medlin, W.L., Schmitt, D.P., [1994] Fracture diagnostics with tube-wave reflections logs. Journal of Petroleum Technology, March, 239-248.

Paige, R.W., Murray, L.R., and Roberts, J.D.M. [1995] Field applications of hydraulic impedance testing for fracture measurements. SPE Production and Facilities, February, 7-12.

Tang, X. M., and Cheng, C. H., [1993] Borehole Stoneley waves propagation across permeable structures. Geophysical Prospecting, 41, 165-187.

Tezuka, K., Cheng, C. H., and Tang, X. M. [1997] Modeling of low-frequency Stoneley-wave propagation in an irregular borehole. Geophysics, 62, 1047-1058.

White, J. E. [1983] Underground sound, Elsevier.

Winkler, K. W., Liu, H., and Johnson, D. L. [1989] Permeability and borehole Stoneley waves: Comparison between experiment and theory. Geophysics 54, 66–75.

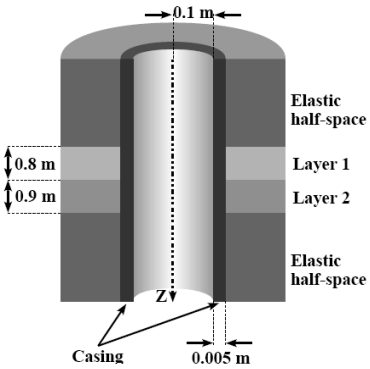

Figure 1: Model 1: cased borehole intersects two elastic layers embedded between two elastic half-spaces

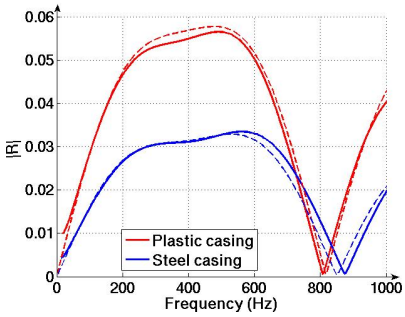

Figure 2: Reflection of tube wave in Model 1 for two cases: plastic casing (red line) and steel casing (blue line). Solid lines indicate coefficients obtained numerically with finite-difference code, while dashed lines represent results of 1D effective wavenumber approach.

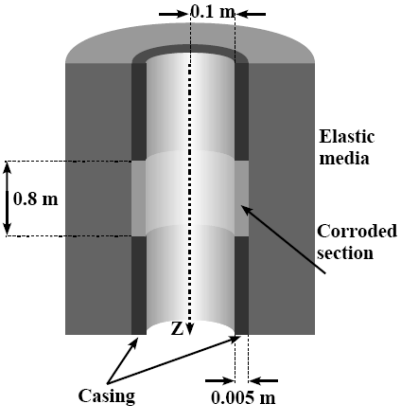

Figure 3: Model 2: cased borehole in homogeneous elastic media; middle section of casing with 0.8 m height is corroded.

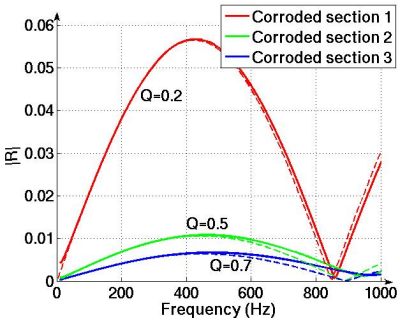

Figure 4: Reflection of tube wave from three different types of corroded section: the highest reflection corresponds to the maximum difference between parameters of casing and corroded region.

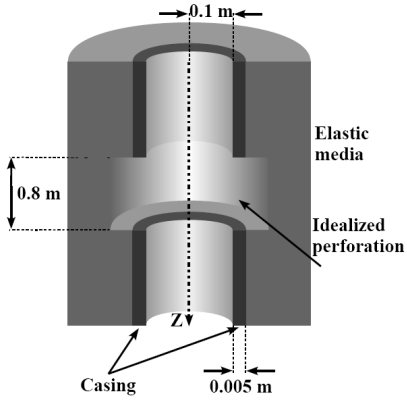

Figure 5: Model 3: Idealized model of a disk-shaped perforation (with no-flow at the sand face).

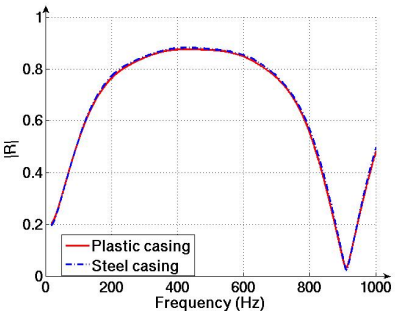

Figure 6: Reflection of tube wave from perforation with 10 cm length for two cases: plastic casing (red line) and steel casing (blue line).

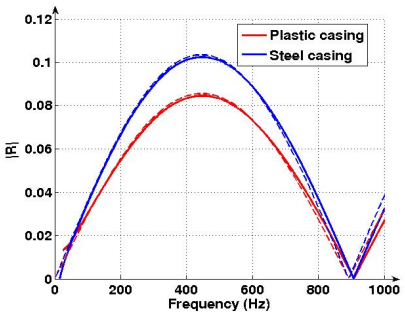

Figure 7: Reflection of tube wave from zero-length perforation for two cases: plastic casing (red line) and steel casing (blue line). Solid lines - finite difference code; dashed lines – 1D effective wavenumber approach.